Synthesis from Caffeine of a Mixed *N*-Heterocyclic Carbene−Silver Acetate Complex Active against Resistant Respiratory Pathogens

Aysegul Kascatan-Nebioglu,[†] Abdulkareem Melaiye,[†] Khadijah Hindi,[†] Semih Durmus,[†] Matthew J. Panzner,[†] Lisa A. Hogue,[‡] Rebekah J. Mallett,[‡] Christine E. Hovis,[‡] Marvin Coughenour,[‡] Seth D. Crosby,[‡] Amy Milsted,[§] Daniel L. Ely,[§] Claire A. Tessier,[†] Carolyn L. Cannon,*[,‡] and Wiley J. Youngs*[,†]

Department of Chemistry, University of Akron, Akron, Ohio 44325-3601, Department of Biology, University of Akron, Akron, Ohio 44325-3908, Division of Allergy and Pulmonary Medicine, Department of Pediatrics, Washington University School of Medicine, St. Louis, Missouri 63110-1002, and Genome Sequencing Center, Washington University School of Medicine, St. Louis, Missouri 63110-1002

Received June 12, 2006

The bis(*N*-heterocyclic carbene) (NHC) silver complex, **3**, with a methyl carbonate anion was formed from the reaction of the iodide salt of methylated caffeine, **1**, with silver (I) oxide in methanol. Attempts to crystallize this complex from a mixture of common alcohols and ethyl acetate led to the formation of an NHC-silver acetate complex, **4**. The more direct synthesis of **4** was accomplished by the in-situ deprotonation of **1** by silver acetate in methanol. Complex **4** demonstrated antimicrobial activity against numerous resistant respiratory pathogens from the lungs of cystic fibrosis (CF) patients including members of the *Burkholderia cepacia* complex that cause a high rate of mortality in patients with cystic fibrosis (CF). Application of this NHC silver complex to primary cultures of murine respiratory epithelial cells followed by microarray analysis showed minimal gene expression changes at the concentrations effective against respiratory pathogens. Furthermore, methylated caffeine without silver showed some antibacterial and antifungal activity.

Introduction

Silver has been used in a variety of ways to control infections since ancient times.[1] Low concentrations of silver ions kill or suppress the activity of a wide range of bacteria and fungi. This activity underlies the efficacy of silver containing products used in the treatment of burns and wounds.[2] The therapeutic use of silver is well-known in the form of inorganic salts and complexes, such as silver nitrate and silver sulfadiazaine and in combination with proteins. Elemental silver has also been used in the form of foils and nanocrystalline particles which can be found in recently developed silver-coated dressings.[3,4]

Silver itself has low toxicity and medically has only one rare cosmetic side effect.[5] The toxicity of silver compounds can often be linked to the carrier molecules underscoring the importance of coordination of silver to other nontoxic molecules for safe use as antimicrobials. Biologically relevant molecules known to have minimal in vivo toxicity, such as xanthine derivatives, may be excellent candidates for this purpose.

We are interested in the synthesis of silver xanthine complexes that have the potential to be used as a new class of antibiotics, particularly for the treatment of lung infections seen in cystic fibrosis (CF[a]) patients. CF is a life threatening genetic disorder which results from mutations in the cystic fibrosis transmembrane regulator (CFTR) gene and affects approximately 60 000 people worldwide. Chronic pulmonary infections with *Pseudomonas aeruginosa*, *Staphylococcus aureus* and *Burkholderia cepacia* complex (Bcc) organisms cause most of the morbidity and mortality in patients with CF.[6]

Xanthines have been used medicinally as diuretics, central nervous system stimulants and inhibitors of cyclic adenosine monophosphate (cAMP) phosphodiesterase resulting in airway smooth muscle relaxation.[7] Caffeine is one xanthine derivative that is readily available and has low toxicity, and thus, is a good candidate for a carrier molecule for the delivery of silver cations to the lungs. Furthermore, the presence of the methylimidazole moiety in the structure of caffeine makes it a valuable candidate for the synthesis of an *N*-heterocyclic carbene (NHC). NHCs are known for their relatively easy syntheses and particularly strong binding ability to main group and transition metals.[8] Two recent reviews discuss the binding of NHCs to silver.[9]

The first step in the synthesis of an NHC silver complex from caffeine is to obtain an imidazolium salt precursor, such as 1,3,7,9-tetramethylxanthinium, also known as methylated caffeine **1**.[10] Previously, our group has reported the synthesis of methylated caffeine with various counterions, and the formation of its biscarbene silver complexes by in situ deprotonation with silver oxide.[11] The use of silver oxide to deprotonate imidazolium salts is one of the most common procedures used for the synthesis of NHC silver complexes.[12] We have also shown the effective antimicrobial properties of NHC silver complexes obtained by this method.[13] Herein we report the synthesis and characterization of the methylated caffeine **1** and silver complexes **3** and **4** derived from **1** and the antimicrobial properties of **1** and **4**.

Results and Discussion

Methylated caffeine, 1,3,7,9-tetramethylxanthinium iodide, **1**, was synthesized by refluxing caffeine with an excess of methyl iodide in DMF using a modified literature procedure (Scheme

* To whom correspondence should be addressed. Phone: 314-286-2954 (C.L.C.); 330-972-5362 (W.J.Y.). Fax: 314-286-2895 (C.L.C.); 330-972-7370 (W.J.Y.). E-mail: cannon_c@kids.wustl.edu (C.L.C.); youngs@uakron.edu (W.J.Y.).

[†] Department of Chemistry, University of Akron.

[‡] Washington University School of Medicine.

[§] Department of Biology, University of Akron.

[a] Abbreviations: NHC, *N*-heterocyclic carbene; CF, cystic fibrosis; CFTR, cystic fibrosis transmembrane regulator; Bcc, *Burkholderia cepacia* complex; QAC, quaternary ammonium compounds; DMF, dimethyl formamide; ESI-MS, electrospray ionization mass spectrometry; MIC, minimum inhibitory concentration; M−H, Mueller−Hinton; LB, Luria broth; SEM, scanning electron microscopy; TEM, transmission electron microscopy; MTECs, murine tracheal epithelial cells; MEEBO, mouse exonic evidence based oligonucleotide; LD_{50}, 50% lethal concentration; NCCLS, National Committee for Clinical Laboratory Standards.

10.1021/jm060711t CCC: $33.50
Published on Web 10/20/2006

Scheme 1. Synthesis of **1**

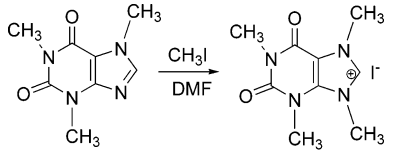

1

1).[10b] Compound **1** is a water-soluble solid and stable in air up to its melting point. In the ^{1}H NMR spectrum, the imidazolium proton appears at 9.30 ppm, which is consistent with the general C−H acidic proton shift of imidazolium salts ($\delta = 8-10$ ppm).[8] The imidazolium carbon appears at 139.6 ppm as the most notable feature in the ^{13}C NMR spectrum.

Compound **1** was combined with an excess amount of silver oxide in methanol. In the ^{1}H NMR spectrum of the product, the lack of the resonance of the imidazolium proton and the downfield shifted methyl protons were observed as indications for the formation of an NHC silver complex. However, the carbene carbon resonance, which is one of the most notable features for the formation of an NHC silver complex in the ^{13}C NMR, was not observed. This can be attributed to the dynamic behavior of the complex in solution as well as the poor relaxation of the quaternary carbene carbon.[9] There are several NHC silver complexes which exhibit this behavior that have been reported in the literature.[9] ESI− MS data showed the bis-(NHC) silver molecular cation at mass 523.1 and its related fragments in the positive mode but the iodide was not observed in the negative mode. The single crystals grown from a concentrated methanol solution of this complex showed the formation of methyl carbonate anion, **3**. This can be explained by the reaction of carbon dioxide in air with the methoxide created in the silver oxide methanol mixture (Scheme 2). There are several literature examples that show bases promote the reaction of primary alcohols with carbon dioxide to give organic carbonates in high yields.[14]

When **3** was dissolved in ethanol, methanol or water and ethyl acetate, and the solvent mixture slowly allowed to evaporate, complex **4** was formed. This complex attracted our attention for several reasons. Complex **4** is composed of biologically relevant ligands, is water soluble and has good stability. These properties make **4** a viable candidate for use as an internal antimicrobial. Furthermore, **4** is a relatively small molecule and may be able to diffuse into the bacteria trapping thick mucus layer in the lungs of CF patients better than conventional larger antibiotics.[15] Complex **4** is a water soluble and light stable solid. For these reasons we explored the direct synthesis of **4**. In situ deprotonation of **1** with silver acetate[16] in 1:2 ratio in methanol gave complex **4** (Scheme 3). The disappearance of the resonance for the imidazolium proton of **1** and the appearance of the resonance for the carbene carbon atom at 186.2 ppm together with carbonyl and methyl carbons of the acetate group at 176.2 and 23.1 ppm, respectively showed the formation of the expected NHC silver acetate complex.

Single-crystal X-ray diffraction data was collected for all synthesized compounds. Single crystals of **1** were obtained by slow evaporation of a concentrated acetonitrile solution (Figure 1). Crystals of **3** suitable for single-crystal X-ray diffraction studies were grown from a concentrated sample in methanol (Figure 2). The asymmetric unit contains the biscarbene methylated caffeine silver complex, a methyl carbonate anion and three solvent methanol molecules. The cation of complex **3** is a planar with an average silver carbene bond distance of 2.094(4) Å. The carbene-Ag-carbene bond angle is 170.83(15)° which deviates significantly from the linear geometry expected for the complex.

Scheme 2. Formation of **3** and **4**

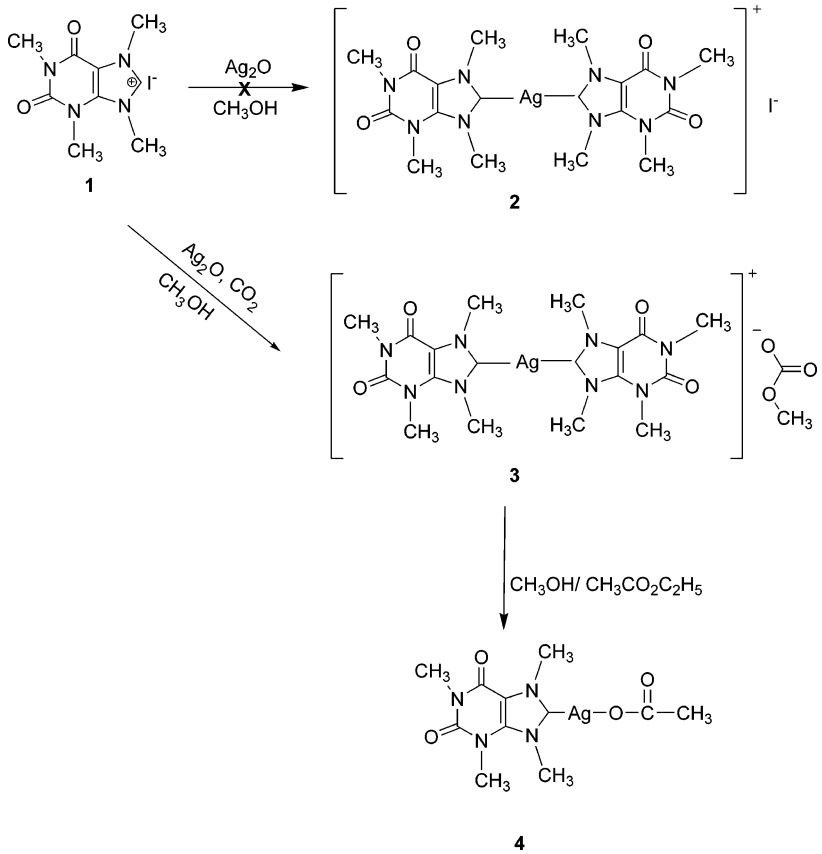

1 **2** **3** **4**

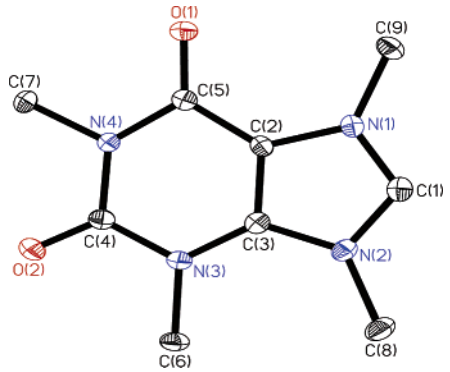

Figure 1. Molecular structure of the cationic part of **1**. Hydrogen atoms have been omitted for clarity.

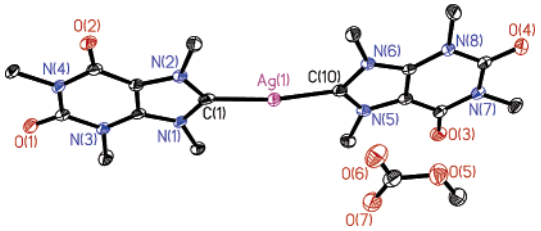

Figure 2. Molecular structure of **3**. Hydrogen atoms have been omitted for clarity.

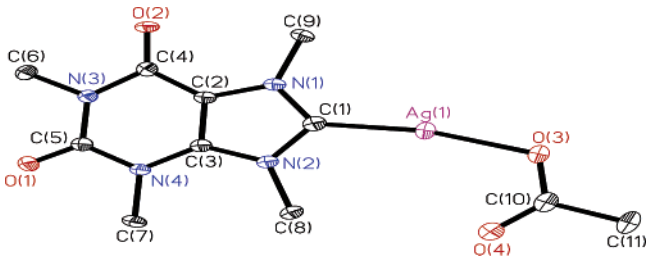

Figure 3. Molecular structure of **4**. Hydrogen atoms have been omitted for clarity.

Scheme 3. Direct Synthesis of **4**

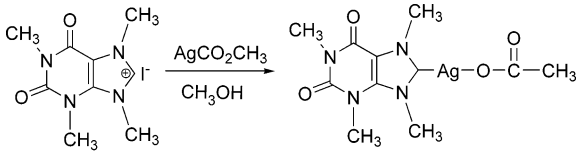

1 **4**

Table 1. Selected Bond Lengths and Angles for **1**, **3**, and **4**

bond lengths and angles	**1**	**3**	**4**
N1−C1	1.317(2) Å	1.378(5) Å	1.343(3) Å
N2−C1	1.349(2) Å	1.334(5) Å	1.376(3) Å
N1−C1−N2	110.77(13)°	105.5(3)°	105.5(2)°
C1−Ag1		2.096(4) Å	2.067(3) Å
C1−Ag1−C10		170.83(15)°	
C1−Ag1−O3			168.19(9)°

Colorless crystals of **4** were obtained from a concentrated sample in a methanol/ethyl acetate mixture (Figure 3). The asymmetric unit of this molecule contains the complex together with two molecules of water. The geometry around the silver atom deviates significantly from linearity with a C1−Ag1−O3 bond angle of 168.19(9)°. The Ag-carbene bond length, 2.067-(3) Å in **4**, is shorter than those in complex **3** (Table 1).

The in vitro antimicrobial activity of methylated caffeine and its silver complex was evaluated against bacterial and fungal strains. The test organisms included *Escherichia coli* and *Pseudomonas aeruginosa* as representative gram-negative bacteria, and *Staphylococcus aureus* as a gram-positive bacterium. *Candida albicans*, *Aspergillus niger* and *Saccharomyces cerevisiae* were used as the representative fungi. Methylated caffeine 1 itself had a bacteriostatic effect on the chosen bacteria with minimal inhibitory concentrations (MIC) of 100 mg/mL for *S. aureus* and 50 mg/mL for both *E. coli* and *P. aeruginosa* by the broth macrodilution method. The fungistatic MIC values for 1 were found to be 150 mg/mL for *C. albicans* and *S. cerevisiae*, and 75 mg/mL for *A. niger*. Several N,N′-disubstituted imidazolium salts, referred to as quaternary ammonium compounds (QAC), have already been shown to have antimicrobial properties.[17] Caffeine is a base analogue that is known to induce mutations in both fungi and bacteria by directly binding to DNA and through inhibition of normal cell cycle checkpoint functions through incompletely understood mechanisms.[18]

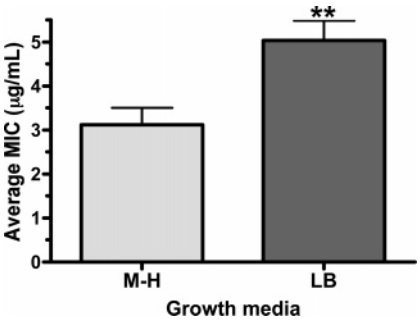

Figure 4. Comparison of the MIC determinations in M−H broth versus LB of the pathogens tested in Table 2, excluding the *E. coli* control organisms, shows a statistically significant difference (two-tailed t test, $^{**}p = 0.0045$, $n = 34$). Data are displayed as mean and SEM (Prism 4, GraphPad).

The antimicrobial activity of the silver complex, **4**, was evaluated against a variety of test organisms including a panel of highly resistant opportunistic pathogens recovered, primarily, from the respiratory tract of patients with cystic fibrosis (CF). Using standard NCCLS broth microdilution methods, the MIC of complex **4** was found to range from 1 to 10 μg/mL for all bacterial strains tested (Table 2). As positive and negative controls, the MIC for complex **4** against *E. coli* J53 strains with and without the silver resistant plasmid pMG101 were tested. This plasmid contains open reading frames for *silP*, *silA*, *silB*, *silC*, *silR*, *silS* and *silE* silver resistance genes originally cloned from a silver nitrate resistant burn ward *Salmonella* isolate.[19] The MIC for J53 lacking the plasmid was less than 1 μg/mL, whereas the MIC of **4** for J53 containing pMG101 was greater or equal to 5 mg/mL demonstrating again, that the antimicrobial activity of complex **4** is primarily due to the silver moiety.

The silver complex **4** was also found to be a very effective antimicrobial agent when tested on fungi. Against *A. niger* and *S. cerevisiae*, **4** was found to be effective with a fungicidal MIC values of 13 μg/mL and 4 μg/mL. It shows a fungistatic effect on *C. albicans* with a MIC value of 4 μg/mL.

The activity of complex **4** against the panel of respiratory pathogens tested in Table 2 varied with the growth media of the bacteria (Figure 4). The mean MIC of complex **4** for this group of pathogens grown in Mueller-Hinton (M−H) was 3.1 ± 0.4 μg/mL (SEM), whereas the mean MIC for the same bacteria grown in Luria broth (LB) was 5.0 ± 0.5 μg/mL (SEM). This difference in MIC was not due to differences in the growth rate of the tested bacteria in the two different enriched media (data not shown). Rather, the differences may be due to differences in the free Ag^+ concentration in each of the media.

Table 2. Microdilution MIC Testing of Complex **4**

genomovar	species name	strain	MIC (μg/mL) M−H	MIC (μg/mL) LB	notes
	Pseudomonas aeruginosa	27853-ATCC	4	10	NCCLS quality control strain[a]
		PAO1−V	4	4	laboratory strain, genome sequenced[b]
		6294	6	6	invasive corneal clinical isolate[b]
		2192	4	2	mucoid CF clinical isolate[b]
		PAM57−15	2	4	mucoid CF clinical isolate[c]
		FRD1	1	10	mucoid CF clinical isolate[b]
		324	1	6	mucoid CF clinical isolate[b]
		1061	1	8	nonmucoid CF clinical isolate[b]
		N6	1	10	nonmucoid CF clinical isolate[b]
		N8	1	6	nonmucoid CF clinical isolate[b]
		N13	1	6	nonmucoid CF clinical isolate[b]
		PAJG3	1	8	nonmucoid CF clinical isolate[b]
	Escherichia coli	J53	1	4	susceptible strain[g]
		J53+pMG101	>5000	>5000	+plasmid with silver resistance genes[g]
		Burkholderia cepacia Complex			
I	*B. cepacia*	PC783	6	6	standard Bcc panel strain[d]
II	*B. multivorans*	HI2229	6	10	standard Bcc panel strain[d]
		AU8170	2	4	CF clinical isolate[e]
		AU5735	8	2	CF clinical isolate[e]
		AU 7484	6	2	CF clinical isolate[e]
		AU5248	2	2	CF clinical isolate[e]
III	*B. cenocepacia*	HI2718	6	4	standard Bcc panel strain[d]
		J2315	1	4	epidemic strain, genome sequenced[d]
		ATTC BAA-245	1	4	LMG 16656, UK CF patient, 1989[a]
IV	*B. stabilis*	HI2210	2	2	standard Bcc panel strain[d]
		ATTC BAA-67	1	1	LMG 14294, Belgium CF pt, 1993[a]
V	*B. vietnamiensis*	PC259	4	4	standard Bcc panel strain[d]
VI	*B. dolosa*	AU0645	4	8	standard Bcc panel strain[d]
		ATTC BAA-246	1	4	LMG 18941, 1st CF *B. dolosa* isolate[a]
		AU4459	6	4	CF clinical isolate[f]
		AU5404	6	4	CF clinical isolate[f]
		AU4881	1	4	CF clinical isolate[f]
		AU9248	1	2	CF clinical isolate[f]
		AU4894	1	4	CF clinical isolate[f]
VII	*B. ambifaria*	HI2468	6	6	standard Bcc panel strain[d]
VIII	*B. anthina*	AU1293	4	4	standard Bcc panel strain[d]
IX	*B. pyrrocinia*	BC11	4	4	standard Bcc panel strain[d]

[a] Strain kindly provided by American Type Culture Collection. [b] Strain kindly provided by Dr. Gerald Pier, Boston, MA. [c] Strain kindly provided by Dr. Thomas Ferkol, St. Louis, MO. [d] Strain kindly provided by Dr. John LiPuma, Ann Arbor, MI. [e] Strain kindly provided by St. Louis Children's Hospital, Clinical Microbiology. [f] Strain kindly provided by Dr. Johannes Huebner, Boston, MA. [g] Strain kindly provided by Dr. Simon Silver, Chicago, IL.

Both M−H and LB are high ionic strength enriched media with reported conductivities of 102 and 112, respectively.[20] The antimicrobial activity of the aminoglycoside antibiotics is known to be exquisitely sensitive to the nature of the media used to determine the MIC[21,22] with high ionic strength media acting to antagonize aminoglycoside activity. Although not documented, one hypothesis used to explain the observed differences in MICs in different media may be due to differences in the activity of efflux pumps that extrude the aminoglycosides.[20] Unidentified Ag^+ efflux pumps in these respiratory pathogens may exhibit different activity in M−H versus LB. If such pumps exist, they may underlie the unstable silver sulfadiazine resistance seen in reported resistant burn ward *P. aeruginosa* isolates.[23,24] Analogous P-type ATPase pumps have recently been identified that allow adaptation to copper stress by *P. aeruginosa*.[25] Alternatively, the differences in MIC may be due to differences in either stability of the complex **4** molecule in each environment causing different rates of Ag^+ release, or differences in complexation of Ag^+ to protein components of the different media. Whatever the explanation, the observed differences are modest and do not predict large differences in MIC in the in vivo setting.

The mechanism of action of complex **4** is currently unknown, as is the mechanism of action of silver cations. To begin to understand the mechanism of its antimicrobial effects, complex **4** was applied to *B. dolosa* and transmission electron microscopy of the treated bacteria was compared with untreated cells. The complex **4** treated bacteria demonstrated disruption of the bacterial cell morphology characterized by cell "ghosts" devoid of cytoplasm. The "ghost" cell membranes were studded with numerous electron dense clusters likely representing outer membrane deposition of silver salts (Figure 5), as has been reported by Sondi and Salopek-Sondi after treatment of *E. coli*

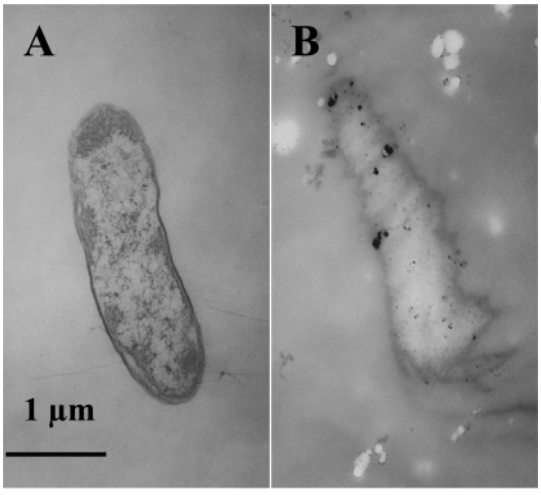

Figure 5. Effects of complex **4** on respiratory pathogens. TEM of *B. dolosa* strain AU4459 before (**A**) and after (**B**) application of 5 μg/mL complex **4** in Luria broth for 1 h at 37 °C.

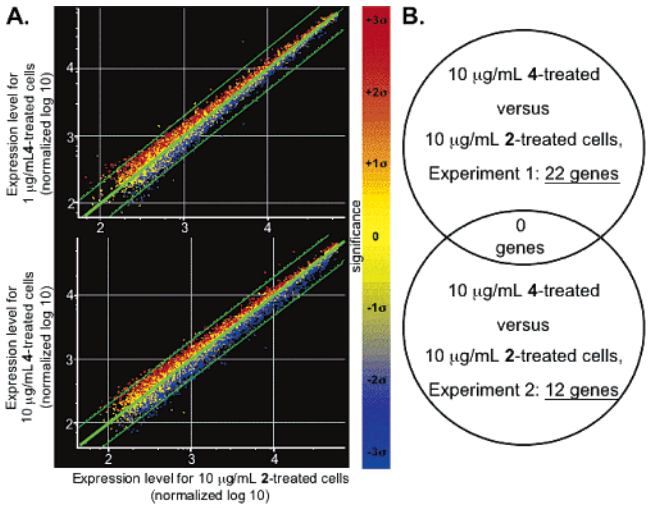

Figure 6. Transcriptional profiling of murine tracheal epithelial cells (METCs) treated with complex **4** shows no significant gene expression changes. Murine tracheal epithelial cells (MTECs) isolated from C57Bl/6 animals and grown to confluency on Transwells were incubated with the indicated concentration of either the methylated caffeine parent compound **2** or the silver complex **4** for 24 h. The RNA was harvested and the cDNA was synthesized and labeled. The labeled cDNA was hybridized to the MEEBO (mouse exonic evidence based oligonucleotide) collection of probes[27] representing over 25 000 mouse genes printed on glass slides. The slides were scanned and intensity values imported into GeneSpring 7.2 software for analysis. The intensity values correlate with expression levels of individual genes, which are displayed as dots on the log-scale scatter plots (**A**) that compare the expression level of each gene in the cells treated with either 1 μg/mL or 10 μg/mL complex **4** versus 10 μg/mL compound **2**. The 10 μg/mL complex 4 treatment induced statistically significant ($p < 0.05$) change in expression of ≥2-fold in only 22 genes. These gene expression changes were not reproduced in a second experiment, which showed changes in only 12 genes, all of which were different from the 22 found in the first experiment (**B**). Of the genes showing expression changes, most were repressed.

with silver nanoparticles.[26] The jagged edges of the cell in the complex **4** treated bacteria may indicate breakdown of the structural integrity of the cell membrane or may simply be an artifact of the sectioning for TEM. Even if partially an artifact, none of the untreated cells exhibited this morphology implicating an effect of the complex **4** treatment.

Preliminary in vitro toxicity studies were performed on primary cultures of murine tracheal epithelial cells (MTECs) in order to test the potential transcriptional effects of the Ag^+ component of complex **4** as a nebulized antimicrobial as compared to those of the carrier compound **1**. In the first experiment, MTEC cultures were incubated for 24 h with either 1 or 10 μg/mL complex **4**, or 10 μg/mL compound **1** dissolved in media. The MTEC cells were lysed, RNA isolated, labeled (Genisphere A350) and samples to be compared were co-hybridized to microarray slides containing probes which represented the entire mouse transcriptome to allow for transcriptional profiling. The pairs of samples applied to the arrays were 1 μg/mL complex **4** co-hybridized with 10 μg/mL compound **1** and 10 μg/mL complex **4** co-hybridized with 10 μg/mL compound **1** with technical replicate per sample pair after dye swapping. Of the few genes that demonstrated >2-fold expression difference (Figure 6A) 5 genes and 22 genes out of a possible 25K were significantly ($p<0.05$) disregulated within the first and second pairs of samples, respectively. There was no overlap between these two sets of genes (Figure 6B). We performed a second experiment to produce a biological replicate and to look for effects at higher concentrations of complex **4**. MTECs were incubated with either 10 μg/mL complex **4** again, 100 μg/mL complex **4** or 10 μg/mL compound **1**, lysed, RNA isolated and labeled with a more sensitive dendrimer system (Genisphere A900) before co-hybridization to the spotted arrays. The 10 μg/mL complex **4** co-hybridized with 10 μg/mL compound **1** pair exhibited only 12 genes with expression changes greater than 2-fold. None of these 12 genes corresponded to any of the 22 genes that were seen in the first experiment with the same concentration pair of **1** and **4** (Figure 6B). The 100 μg/mL complex **4** co-hybridized with 10 μg/mL compound **1** pair resulted in 2-fold expression changes in 81 genes. One gene, Trim30 (Genbank NM_009099), was down regulated in this latter pairing (fold change 0.39), as well as in the first experiment 10 μg/mL complex **4** versus 10 μg/mL compound **1** pair (fold change 0.49). However, this same gene was noted to be down regulated in a 10 μg/mL methylated caffine compound **1** versus media alone pair (fold change 0.397) and thus, is most likely due to an effect of the parent compound on respiratory epithelial cells rather than an effect of silver cations. Thus, silver treatment of MTECs caused no significant consistent transcriptional change at any concentration tested. Nor were there any dose responsive genes among the small, likely insignificant, number that did appear to be >2-fold altered.

Preliminary toxicity studies on a small number of rats showed that methylated caffeine, **1**, administered intravenously, has low toxicity with an LD50 (50% lethal concentration) of 1068 mg/kg. The kidneys, livers, adrenals and hearts of the experimental rats appeared normal upon autopsy. A study using the silver complex **4** was also performed. Because **4** decomposes in the presence of chloride ions, it was dissolved in water instead of saline. The amount injected was limited due to the solubility of the complex in water, which is 11.6 mg/mL. No adverse effects were noted after the injections.

Conclusion

We have synthesized a novel mixed N-heterocyclic carbene-acetate complex of silver from caffeine. We determined that both the silver complex and the methylated caffeine parent compound exhibit antimicrobial properties. In addition to its antifungal activity and activity against selected gram-negative and gram-positive bacteria, the NHC silver complex derived from methylated caffeine demonstrated antimicrobial activity against numerous resistant respiratory pathogens including members of the *Burkholderia cepacia* complex. Transcriptional profiling of murine tracheal epithelial cells treated with the silver complex and the methylated caffeine parent compound showed no significant gene expression changes. Preliminary in vivo toxicity studies demonstrated very low toxicity for both the parent methylated caffeine and the silver complex. Given the water solubility of this silver complex and its low toxicity, it may prove useful as a nebulized therapy in patients colonized with these resistant organisms. We are currently exploring the synthesis of other silver xanthine complexes having different groups on the imidazole ring to enable higher water solubility.

Experimental Section

General Methods. All manipulations were carried out in air. Caffeine and methyl iodide were purchased from Acros. Silver acetate was purchased from Aldrich. ^{1}H and ^{13}C NMR data were recorded on a Gemini 300 MHz instrument and were referenced to residual protons and ^{13}C signals of deuterated solvents. ^{109}Ag NMR data was recorded on a Unity Inova 750 MHz instrument and $AgNO_3$ in d_6-DMSO was used as an external reference. Mass spectrometry data were collected on a Bruker Daltons (Billerica,

MA) Esquire-LC mass spectrometer equipped with ESI. LB Broth, Miller and Bactor agar were purchased from DIFCO.

Technical Details of the X-ray Structure Determinations. Crystal of **1**, **3** and **4** were coated in paraffin oil, mounted on a kryo loop and placed on a goniometer under a stream of nitrogen. X-ray data sets were collected on a Bruker Apex CCD diffractometer with graphite-monochromated Mo Kα radiation (λ = 0.71073 Å). Unit cell determination was achieved by using reflections from three different orientations. An empirical absorption correction and other corrections were done using multiscan SADABS. Structure solution, refinement and modeling were accomplished using the Bruker SHELXTL package.[28] The structure was obtained by full-matrix least-squares refinement of F^2 and the selection of appropriate atoms from the generated difference map.

Synthesis of 1,3,7,9-tetramethylxanthinium iodide. (1) Caffeine (9.00 g, 46.4 mmol) was refluxed with methyl iodide (15 mL) in *N*, *N*′-dimethyl formamide (50 mL) at 145 °C for 20 h. An excess amount of acetone was added to the clear solution obtained and the precipitate filtered and washed with acetone. Crystallization from acetonitrile gave **1** as a yellowish white solid (19.4 mmol, 6.52 g, 42%). Mp: 187−190 °C. Anal. Calcd for $C_9H_{13}IN_4O_2 \cdot H_2O$: C, 30.52; H, 4.27; N, 15.82. Found: C, 30.27; H, 4.18; N, 15.41. ^{1}H NMR (300 MHz, d_6-DMSO): δ 9.30 (s, 1H, NCHN), 4.16 (s, 3H, CH_3), 4.06 (s, 3H, CH_3), 3.75 (s, 3H, CH_3), 3.28 (s, 3H, CH_3). ^{13}C {^{1}H} NMR (75 MHz, d_6-DMSO): δ 153.3 (C═O), 150.2 (C═O), 139.6 (NCHN), 139.3(C═C), 107.8 (C═C), 36.9, 35.6, 31.4, 28.4 (NCH_3). ESI-MS (*m*/*z*): 209 [$C_9H_{13}N_4O_2^+$]. X-ray crystal structure analysis of **1**: formula $C_9H_{15}IN_4O_3$, *Mw* = 354.15, colorless crystal 0.40 × 0.40 × 0.30 mm, a = 7.8807(5) Å, b = 8.1331(6) Å, c = 10.8982(7) Å, α = 96.4480(10)°, β = 99.4090(10)°, γ = 110.5710(10)°, V = 634.19(7) Å^3, Dcalc = 1.855 Mg.m^{-3}, μ = 2.529 mm^{-1}, Z = 2, triclinic, space group P-1, λ = 0.71073 Å, T = 100 K, ω and φ scans, 5638 reflections collected, 2944 independent (R_{int} = 0.0123), 166 refined parameters, R1/*w*R2 ($I \geq 2\sigma(I)$) = 0.0148/ 0.0372 and R1/wR2 (all data) = 0.0152/ 0.0374, maximum (minimum) residual electron density 0.465(−0.291) e.Å^{-3}.

Synthesis of bis(1,3,7,9-tetramethylxanthine-8-ylidene)silver methyl carbonate. (3). 1 (0.68 g, 2.0 mmol) was dissolved in methanol (72 mL) and Ag_2O (0.70 g, 3.0 mmol) was added. The mixture was stirred at room temperature in the dark for 2 h 25 min. The dark gray suspension was filtered to give a colorless solution. The volatiles were removed in vacuo. Compound **3** (0.55 g, 0.85 mmol, 85%) was obtained as a brownish solid. Mp: 120−123 °C. Anal. Calcd for $C_{20}H_{27}AgN_8O_7$: C, 40.08; H, 4.54; N, 18.70. Found: C, 39.39; H, 4.57; N, 19.06. ^{1}H NMR (300 MHz, d_6-DMSO): δ 4.20 (s, 6H, CH_3), 4.07 (s, 6H, CH_3), 3.75 (s, 6H, CH_3), 3.31 (s, 2H, H_2O), 3.29 (s, 3H, CH_3), 3.26 (s, 6H, CH_3). ^{13}C {^{1}H} NMR (75 MHz, d_6-DMSO): δ 161.0 (C═O), 152.3 (C═O), 150.4 (C═O), 140.4 (C═C), 108.7 (C═C), 54.4 (CH_3), 36.9, 31.7, 30.2, 27.7 (CH_3). ESI-MS (*m*/*z*): 523.1 [$C_{18}H_{24}AgN_8O_4^+$], 314.8 [$C_9H_{12}AgN_4O_2^+$], 208.9 [$C_9H_{13}N_4O_2^+$]. X-ray crystal structure analysis of **3**: formula $C_{23}H_{39}AgN_8O_{10}$, *Mw* = 695.49, colorless crystal 0.33 × 0.28 × 0.08 mm, a = 8.0385(10) Å, b = 9.1589(12) Å, c = 20.262(3) Å, α = 88.876(2)°, β = 78.611(2)°, γ = 75.225(2)°, V = 1413.3(3) Å^3, Dcalc = 1.634 Mg cm^{-3}, μ = 0.783 mm^{-1}, Z = 2, triclinic, space group *P*-1 (No. 2), λ = 0.71073 Å, T = 100 K, ω and φ scans, 12637 reflections collected, 6599 independent (*R*int) 0.0342), 394 refined parameters, R1/*w*R2 ($I \geq 2\sigma(I)$) = 0.0568/0.1464 and R1/wR2 (all data) = 0.0638/ 0.1512, maximum (minimum) residual electron density 2.330 (−1.920) e Å^{-3}, all hydrogen atoms were calculated and refined as riding atoms.

Synthesis of (1,3,7,9-tetramethylxanthine-8-ylidene)silver-acetate. (4) Compound **1** (4.00 mmol, 1.34 g) was dissolved in methanol (100 mL) and silver acetate (8.00 mmol, 1.34 g) was added. The mixture was stirred at room temperature for 40 min. The yellow silver iodide suspension was filtered to give a colorless solution. The volatiles were removed in vacuo. Compound **4** (1.22 mmol, 0.5 g, 30%) was obtained as a white solid after recrystallization from ethanol. Mp: 209−212 °C. Anal. Calcd for $C_{11}H_{15}AgN_4O_4 \cdot 2H_2O$: C, 32.11; H, 4.62; N, 13.62. Found: C, 31.95; H, 4.33; N, 13.18. ^{1}H NMR (300 MHz, D_2O): δ 4.19 (s, 3H, CH_3), 4.07 (s, 3H, CH_3), 3.82 (s, 3H, CH_3), 3.34 (s, 3H, CH_3), 1.91 (s, 3H, $COCH_3$). ^{13}C {^{1}H} NMR (75 MHz, DMSO): δ 186.2 (C−Ag), 176.2 (C═O), 153.9 (C═O), 151.3 (C═O), 141.2 (C═C), 109.6 (C═C), 39.3, 37.8, 31.4, 29.7 (N−CH_3), 23.1 ($COCH_3$). ^{109}-Ag NMR: 409.53 (broad C−Ag). ESI-MS (*m*/*z*): 523 [$C_{18}H_{24}AgN_8O_4^+$], 315 [$C_9H_{12}AgN_4O_2^+$], 209 [$C_9H_{13}N_4O_2^+$]. X-ray crystal structure analysis of **4** (with $2H_2O$ cocrystallized): formula $C_{11}N_4O_6H_{19}Ag$, *Mw* = 411.16, colorless crystal 0.21 × 0.18 × 0.03 mm, a = 8.4027(8) Å, b = 6.2961(6) Å, c = 14.1856(14) Å, α = 90°, β = 98.243(2)°, γ = 90°, V = 742.73(12) Å^3, Dcalc = 1.839 Mg.m^{-3}, μ = 1.393 mm^{-1}, Z = 2, monoclinic, space group $P2_1/m$, λ = 0.71073 Å, T = 100 K, ω and φ scans, 6661 reflections collected, 1940 independent (R_{int} = 0.0200), 150 refined parameters, R1/*w*R2 ($I \geq 2\sigma(I)$) = 0.0244/0.0598 and R1/wR2 (all data) = 0.0256/0.0604, maximum (minimum) residual electron density 1.593 (−0.229) e.Å^{-3}.

In vitro antimicrobial activity. The MIC was determined by both the broth macro- and micro-dilution methods. For the macrodilution MIC testing of fungi, 5 mL of sterilized LB broth was inoculated with stationary phase fungi and grown for 72 h at room temperature without shaking. Serial dilutions of freshly prepared **1** or **4** in culture tubes were inoculated with a constant volume of the cultures of fungi and incubated for 72 h at room temperature. The MIC was determined by visual inspection of the tubes for growth.

The micro-broth dilution MIC determination was performed using a standard NCCLS protocol.[29] Bacteria are streaked from glycerol-frozen stocks onto blood agar plates and incubated overnight at 37 °C. Cells from the fresh plates are suspended in either Luria broth or the NCCLS standard Mueller-Hinton broth to an OD_{650} of 0.25 and grown in a shaking incubator until the OD_{650} is 0.4, which corresponds to ∼2 × 10^8 CFU/mL, confirmed by plating serial dilutions. The bacteria are diluted in broth to a concentration corresponding to 10^5 CFU in 100 μL, which is added to triplicate well of a 96 well plate containing 100 μL of the complex **4** concentration to be tested. The plate is incubated for 18 h at 37 °C and MIC determined as the lowest concentration with clear wells.

Cell Culture. We used a modification of the method published by You and colleagues to isolate primary murine airway epithelial cells and establish cultures.[30] Briefly, immediately after CO_2 euthanasia of the C57Bl/6J mice, tracheae were isolated and collected in Ham's F-12 medium with 100 U/ml penicillin and 100 μg/mL streptomycin (Ham's F-12/pen-strep) held at 4 °C. Each trachea was stripped of overlying tissue, cut lengthwise and rinsed twice with Ham's F-12/pen-strep. Tracheae were placed in a clean 15 mL tube, Pronase (Roche Molecular Biochemicals, Indianapolis, IN) was added (0.15%) to Ham's F-12/pen-strep and the tracheae were incubated overnight at 4 °C. The tube was gently inverted several times to dislodge cells. Fetal calf serum (10%) was added to halt enzymatic digestion prior to more gentle agitation and wash steps to release cells. The cell suspensions pooled from all of the animals were pelleted at ∼400 g for 10 min at 4 °C, resuspended in Ham's F-12/pen-strep with 0.5 mg/mL crude pancreatic DNase I (Sigma-Aldrich) and incubated on ice for 5 min followed by centrifugation at ∼400 g for 5 min at 4 °C. Removed the supernatant and resuspended the cells in 1:1 DMEM:Ham's F12 medium (vol: vol) with 100 U/ml penicillin, 100 μg/mL streptomycin, 0.25 μg/mL fungizione, 15 mM HEPES, 4 mM L-glutamine and 3.6 mM $NaHCO_3$ (MTEC Basic medium) supplemented with 10 μg/mL insulin, 5 μg/mL transferrin, 0.1 μg/mL cholera toxin, 25 ng/mL epidermal growth factor (Becton-Dickinson, Bedford, MA), 30 μg/mL bovine pituitary extract and 5% fetal calf serum. The resuspended cells were seeded at low density on semipermeable membranes (Transwell) of 6 well plates coated with collagen. Approximately 4 × 10^5 cells, recovered from ∼2 trachea, were seeded per individual well, which were then placed in a humidified incubator at 37 °C in 5% CO2 for 7 days. After the cells established tight junctions and a high trans-membrane resistance (>1000 mOhms·cm2), media was removed from the upper chamber, along with any nonadherent cells and debris, to create an air−liquid

interface (ALI). The medium in the bottom chamber was also removed, and replaced with MTEC Basic medium supplemented with 2% NuSerum(Becton-Dickinson) and 10^{-8} M retinoic acid. The medium was replaced twice weekly. Primary cultures remained viable for up to 80 days. Cells became differentiated in this defined media under ALI conditions and developed characteristics of epithelial cells in the airways including a ciliated and nonciliated population. Multiple layers were present including basal cells.

Transmission Electron Microscopy. Bacteria to be examined by transmission electron microscopy (EM) were pelleted, fixed in 2.5% glutaraldehyde in 0.1 M sodium cacodylate for 1 h at 4 °C, washed for 20 min three times in 0.1 M sodium cacodylate, and then incubated with 1.25% osmium tetroxide in PBS for 90 min at 25 °C. Samples were further fixed in 4% uranyl acetate, thin-sectioned (90 nm) in Polybed 812 (Polysciences, Warrington, PA), poststained in uranyl acetate and lead citrate, then visualized on a Zeiss 902 microscope (Zeiss, Thornwood, NY) and recorded on electron microscopy film.

Microarray Gene Expression Analysis. The microarrays used were created from the publically available MEEBO (Mouse Exonic Evidence Based Oligonucleotide) collection of probes representing greater than 25,000 mouse genes[27] (Invitrogen) printed out of 3xSSC with 0.75 M betaine buffer onto epoxysilane slides (Corning). Murine tracheal epithelial cells (MTECs) isolated from C57Bl/6 animals, grown to confluency and allowed to differentiate at an air liquid interface for 21 days were incubated at 37 °C with either methylated caffeine, **1** or complex **4** in 1 mL of media applied to the apical surface for 24 h. The inserts were rinsed with PBS and the total RNA isolated using the RNeasy Mini Kit (Qiagen). The RNA was quantified spectrophotometrically and the RNA quality assured through visualization on glyoxyl gels and analysis on an Agilent bioanalyzer 2100. Starting with 2 or 8 μg of total RNA, first strand cDNA was generated by modified oligo(dT)-primed reverse transcription (Superscript II; Invitrogen) utilizing the 3DNA Array 350 kit or the 3DNA Array 900 kit, respectively (Genisphere). The 3DNA dT primers bear a capture sequence on the 5′ end. Two hybridizations were carried out in a sequential manner. The primary hybridization was performed by adding cDNA to the microarray which was incubated at 63 °C for 16−20 h. A second hybridization was carried out using the fluorescent dendrimers (Genishpere) which contain oligos complementary to the capture sequence in the dT primers. To create technical replicates for each condition, RNAs were divided into two samples. These samples were independently labeled with each dye, either Cy5 or Cy3 to allow for dye-swapping. Thus, two DNA microarrays were scanned for each sample pair tested.

Slides were scanned immediately after hybridization in a PerkinElmer ScanArray Express HT scanner to detect Cy3 and Cy5 fluorescence. Laser power was kept constant for the scans, and photomultiplier tube values were set for optimal intensity with minimal background. The intensity values are imported into GeneSpring 7.2 software (Agilent, Redwood city, CA) for analysis. Local background intensity was subtracted from individual spot intensities. To account for the dye swap, the "signal" channel and "control" channel measurements were reversed in those samples so that signal derived from methylated caffeine-treated RNA occupies the control channel and complex **4** treated RNA the signal channel. A Lowess curve was fit to the log-intensity versus log-ratio plot. 20.0% of the data was used to calculate the Lowess fit at each point. This curve was used to adjust the control value for each measurement. If the control channel was lower than 10 RFU then 10 was used instead. The mean signal to Lowess adjusted controlled ratios were calculated. The cross-chip averages were derived from the antilog of the mean of the natural log ratios across the two microarrays. Oligonucleotide elements derived from mouse elements that received a "present" call (intensity > 200RFU or local signal-to-background > 2 in either channel) by the ScanArray software were identified and all others were excluded from the analysis. Data were filtered using a one-sample T-test ($p<0.05$) and a 2-fold cutoff.

Animal Studies. Male C57/Bl6 mice were housed in the Clinical Sciences Research building animal facility managed by veterinarians associated with Washington University School of Medicine. All procedures involving mice were approved by the Washington University Animal Studies Committee.

Male Sprague Dawley (Harlan Sprague Dawley, Indianapolis, IN) adult rats (500 g average body weight) were housed in the University of Akron animal facility. Temperature and humidity were held constant, and a standard light cycle (12 h light/12 h dark) was used. Food (Lab diet 5P00, Prolab, PMI nutrition, Intl., Bretwood, MO) and water were provided ad libitim. Animals were anesthetized with ether to inject the compound into the tail vein, using a 26 3/8 gauge syringe needle in a volume of 0.3 mL sterile saline. The concentrations of the ligand ranged from 5.3 mg/kg to 1068 mg/kg. At the end dosages of the experiment, animals were terminated, and the liver, lung, kidney, and heart tissues were removed and frozen at −70 °C for 24 h. Urine samples were collected using metabolic cages for later examination of the compound distribution.

Acknowledgment. This work was supported by the University of Akron, the National Science Foundation (CHE0315980) to W.J.Y. and C.A.T., and the National Institutes of Heath through grants to C.L.C. from the National Heart, Lung and Blood Instititute (HL04277), as a Scholar of the Child Health Research Center in Developmental Biology at Washington University School of Medicine (HD01487) and by the National Institute of Allergies and Infectious Diseases (1 R01 A1067856 01). We thank Venkat Dudipala for his assistance in the collection of ^{109}Ag NMR spectra, Daniel J. Smith for providing the metabolic cages and Marilyn Levy for her assistance with the transmission electron microscopy.

Supporting Information Available: Tables giving data and details for the crystal structure determinations of **1**, **3** and **4**.

References

(1) Russel, A. D.; Path, F. R.; Hugo, W. B. Antimicrobial activity and action of silver. *Prog. Med. Chem.* **1994**, *31*, 351−370.
(2) Landsdown, A. B. G. A Review of the use of silver in wound care: Facts and fallacies. *Br. J. Nursing* **2004**, *13*, S6−S19.
(3) Landsdown, A. B. G. Silver(I): Its antibacterial properties and mechanism of action. *J. Wound Care* **2002**, *11*, 125−130.
(4) Lansdown, A. B.; Williams, A. How safe is silver in wound care. *J. Wound Care* **2004**, *13*, 131−136.
(5) (a) Hostynek, J. J.; Hinz, R. S.; Lorence, C. Metals and the skin. *Crit. Rev. Toxicol.* **1993**, *23*, 171−235. (b) Hollinger, M. A. Toxicological aspects of silver pharmeceuticals. *Crit. Rev. Toxicol.* **1996**, *26*, 255−260.
(6) Lyczak, J. B.; Cannon, C. L.; Pier, G. B. Lung infections associated with cystic fibrosis. *Clin. Microbiol. Rev.* **2002**, *15*, 194−222.
(7) Cropp, G. J. Effectiveness of bronchodilators in cystic fibrosis. *Am. J. Med.* **1996**, *100* (1A), 19S−29S.
(8) (a) Herrmann, W. A.; Kocher, C. *N*-Heterocyclic carbenes. Essays on organometallic chemistry. 9. *N*-Heterocyclic carbenes. *Angew. Chem., Int. Ed. Engl.* **1997**, *36*, 2162−2187. (b) Bourissou, D.; Guerret, O.; Gabbaï, F. P.; Bertrand, G. Stable carbenes. *Chem. Rev.* **2000**, *100*, 39−91. (c) Arduengo, A. J., III; Rasika-Dias, H.-V.; Calabrese, J. C.; Davidson, F. Homoleptic carbene−silver(I) and carbene−copper(I) complexes. *Organometallics* **1993**, *12*, 3405−3409. (d) Garrison, J. C.; Tessier, C. A.; Youngs, W. J. Synthesis and crystallographic characterization of multidonor *N*-heterocyclic carbene chelating ligands and their silver complexes: Potential use in pharmaceuticals. *J. Organomet. Chem.* **2005**, *690*, 6008−6020.
(9) (a) Lin, I. J. B.; Vasam, C. S. Silver(I) *N*-heterocyclic carbenes. *Comments Inorg. Chem.* **2004**, *25*, 75−129. (b) Garrison, J. C.; Youngs, W. J. Ag(I) *N*- heterocyclic carbene complexes: Synthesis, structure and application. *Chem. Rev.* **2005**, *105*, 3978−4008.
(10) (a) Paderi, C. Physiological action of 1,3,7,9-tetramethylxanthine hydrate compared with that of caffeine. *Arch. Farmacol. Sper. Sci. Affini* **1926**, *41*, 92−101. (b) Ivanov, E. I.; Kalayanov, G. D.; Yaroshchenko, I. M.; Stepanov, D. E. Novel synthesis of caffeine iodomethylate and its homologues. *Khim. Geterotsikl. Soedin.* **1989**, *11*, 1570−1571.
(11) Kascatan-Nebioglu, A.; Panzner, M. J.; Garrison, J. C.; Tessier, C. A.; Youngs, W. J. Synthesis and structural characterization of *N*-heterocyclic carbene complexes of silver(I) and rhodium(I) from caffeine. *Organometallics* **2004**, *23*, 1928−1931.

(12) Wang, H. M. J.; Lin, I. J. B. Facile synthesis of silver(I)−carbene complexes. Useful carbene transfer agents. *Organometallics* **1998**, *17*, 972−975.
(13) (a) Melaiye, A.; Simons, R. S.; Milsted, A.; Pingitore, F.; Wesdemiotis, C.; Tessier, C. A.; Youngs, W. J. Formation of water-soluble pincer silver(I)−carbene complexes: A novel antimicrobial agent *J. Med. Chem*. **2004**, *47*, 973−977. (b) Melaiye, A.; Sun, Z.; Hindi, K.; Milsted, A.; Ely, D.; Reneker, D. H.; Tessier, C. A.; Youngs, W. J. Silver(I)−imidazole cyclophane gem−diol complexes encapsulated by electrospun tecophilic nanofibers: Formation of nanosilver particles and antimicrobial activity. *J. Am. Chem. Soc*. **2005**, *127*, 2285−2291.
(14) (a) Hirao, I.; Kito, T.; Funamoto, T.; Murakami, T.; Usami, K. Carboxylation of phenol derivatives. XXII. Formation of alkali alkyl carbonate by the *O*-carboxylation of alcohol in the presence of an alkali salt of a weak acid. *Bull. Chem. Soc. Jpn.* **1976**, *49*, 2775−2779. (b) Casadei, M. A.; Cesa, S.; Rossi, L. Electrogenerated-base-promoted synthesis of organic carbonates from alcohols and carbon dioxide. *Eur. J. Org. Chem.* **2000**, 2445−2448. (c) Verdecchia, M.; Feroci, M.; Palombi, L.; Rossi, L. Safe and mild synthesis of organic carbonates from alkyl halides and tetrabutylammonium alkyl carbonates. *J. Org. Chem.* **2002**, *67*, 8287−8289.
(15) (a) Bhat, P. G.; Flanagan, D. R.; Donovan, M. D. Drug diffusion through cystic fibrotic mucus: Steady-state permeation, rheologic properties, and glycoprotein morphology. *J. Pharm. Sci*. **1996**, *85*, 624−30. (b) Wesley, A. W.; Qureshi, A. R.; Forstner, G. G.; Forstner, J. F. Differences in Mucus glycoproteins of small intestine from subjects with and without cystic fibrosis. In *Mucus in Health and Disease*; Chantler, E. N., Elder, J. B., Elstein, M., Eds.; Plenum: New York, 1982; Vol 2, pp 145−161.
(16) Guerret, O.; Solé, S.; Gornitzka, H.; Teichert, M.; Trinquier, G.; Bertrand, G. 1,2,4-Triazole-3,5-diylidene: A building block for organometallic polymer synthesis. *J. Am. Chem. Soc.* **1997**, *119*, 6668−6669.
(17) (a) Janssen, A. P. J.; Heeres, J.; Hermans, H. K. F. Imidazolium Salts. U.S. Patent 3,991,202, 1976. (b) Klötzer, W.; Link, H.; Müssner, R.; Schiestl, W.; Singewald, N. Antimicrobial 1,3-disubstituted/imidazolium salts. U.S. Patent 4,814,332, 1989. (c) Pernak, J., Rogoża, J.; Mirska I. Synthesis and antimicrobial activities of new pyridinium and benzimidazolium chlorides. *Eur. J. Med. Chem.* **2001**, *36*, 313−320. (d) Demberelnyamba, D.; Kim, K.-S.; Choi, S.; Park, S.-Y.; Lee, H.; Kim, C.-J.; Yoo, I.-D. Synthesis and antimicrobial properties of imidazolium and pyrrolidinonium salts. *Bioorg. Med. Chem.* **2004**, *12*, 853−857. (e) Pernak, J.; Sobaszkiewicz, K.; Foksowicz-Flaczyk, J. Liquids with symmetrical dialkoxymethyl-substituted imidazolium cations. *Chem. Eur. J.* **2004**, *10*, 3479−3485.
(18) (a) Osman, F.; McCready, S. Differential effects of caffeine on DNA damage and replication cell cycle checkpoints in the fission yeast *Schizosaccharomyces pombe*. *Mol. Gen. Genet.* **1998**, *260*, 319−334. (b) Abratt, V. R.; Peak, M. J.; Peak, J. G.; Santangelo, J. D.; Woods, D. R. Induction and repair of DNA strand breaks in Bacteroides fragilis. *Can. J. Microbiol.* **1990**, *36*, 490−494. (c) Selby, C. P.; Sancar, A. Mechanisms of caffeine inhibition of DNA repair in *E. coli*. *Prog. Clin. Biol. Res*. **1990**, *340A*, 179−193.
(19) (a) Gupta, A.; Matsui, K.; Lo, J. F.; Silver, S. Molecular basis for resistance to silver cations in Salmonella. *Nat. Med*. **1999**, *5*, 183−188. (b) Silver, S. Bacterial silver resistance: Molecular biology and uses and misuses of silver compounds. *FEMS Microbiol. Rev*. **2003**, *27*, 341−353.
(20) Li, X. Z.; Poole, K.; Nikaido, H. Contributions of MexAB−OprM and an EmrE homologue to intrinsic resistance of *Pseudomonas aeruginosa* to aminoglycosides and dyes. *Antimicrob. Agents Chemother*. **2003**, *47*, 27−33.
(21) Medeiros, A. A.; O'Brien, T. F.; Wacker, W. E.; Yulug, N. F. Effect of salt concentration on the apparent in vitro susceptibility of Pseudomonas and other gram-negative bacilli to gentamicin. *J. Infect. Dis.* **1971**, *124*, Suppl. 56−59.
(22) Rosenberg, E. Y.; Ma, D.; Nikaido, H. AcrD of *Escherichia coli* is an aminoglycoside efflux pump. *J. Bacteriol*. **2000**, *182*, 1754−1756.
(23) Bridges, K.; Kidson, A.; Lowbury, E. J.; Wilkins, M. D. Gentamicin- and silver-resistant pseudomonas in a burns unit. *Br. Med. J*. **1979**, *1*, 446−449.
(24) Pirnay, J. P.; De Vos, D.; Cochez, C.; Bilocq, F.; Pirson, J.; Struelens, M. L.; Duinslaeger, L.; Cornelis, P.; Zizi, M.; Vanderkelen, A. Molecular epidemiology of *Pseudomonas aeruginosa* colonization in a burn unit: Persistence of a multidrug-resistant clone and a silver sulfadiazine-resistant clone. *J. Clin. Microbiol.* **2003**, *41*, 1192−1202.
(25) Teitzel, G. M.; Parsek, M. R. Heavy metal resistance of biofilm and planktonic *Pseudomonas aeruginosa*. *Appl. Environ. Microbiol*. **2003**, *69*, 2313−2320.
(26) Sondi, I.; Salopek-Sondi, B. Silver nanoparticles as antimicrobial agent: A case study on E. coli as a model for Gram-negative bacteria. *J. Colloid Interface Sci.* **2004**, *275*, 177−182.
(27) Functional genomics custom oligos. Mouse exonic evidence based oligonucleotide (MEEBO). http://arrays.ucsf.edu/meebo.html (accessed March, 2006).
(28) Sheldrick, G. M. *SHELX97: Programs for Crystal Structural Analysis*; University of Göttingen, Göttingen, Germany, 1997.
(29) (a) N.C.C.L. Standards, Methods for dilution antimicrobial susceptibility tests for bacteria that grow aerobically, Approved standard; 6th edition and Performance standards for antimicrobial susceptibility testing, 15th Informational Supplement, NCCLS: Baltimore, MD, 2004. (b) Andrews, J. M. Determination of minimum inhibitory concentrations. *J. Antimicrob. Chemother*. **2001**, *48*, 5−16.
(30) You, Y.; Richer, E. J.; Huang, T.; Brody, S. L. Growth and differentiation of mouse tracheal epithelial cells: selection of a proliferative population. *Am. J. Physiol. Lung Cell. Mol. Physiol*. **2002**, *283*, L1315−L1321.

JM060711T